The phase diagram and hidden order for generalized spin ladders

1996 J. Phys.: Condens. Matter 8 7161

(http://iopscience.iop.org/0953-8984/8/38/018)

J. Phys.: Condens. Matter **8** (1996) 7161–7177. Printed in the UK

The phase diagram and hidden order for generalized spin ladders

S Brehmer, H-J Mikeska and U Neugebauer

Institut für Theoretische Physik, Universität Hannover, 30167 Hannover, Germany

Received 18 March 1996

Abstract. We investigate the phase diagram of antiferromagnetic spin ladders with additional exchange interactions on diagonal bonds by variational and numerical methods. These generalized spin ladders interpolate smoothly between the $S = \frac{1}{2}$ chain with competing nn and nnn interactions, the $S = \frac{1}{2}$ chain with alternating exchange and the antiferromagnetic (AF) $S = 1$ chain. The Majumdar–Ghosh ground states are formulated as matrix product states and are shown to exhibit the same type of hidden order as the AF $S = 1$ chain. Generalized matrix product states are used for a variational calculation of the ground state energy and the spin and string correlation functions. Numerical (Lanczos) calculations of the energies of the ground state and of the low-lying excited states are performed, and compare reasonably with the variational approach. Our results support the hypothesis that the dimer and Majumdar–Ghosh points are in the same phase as the AF $S = 1$ chain.

1. Introduction

In the last few years spin systems consisting of a finite number n of interacting spin chains with $S = \frac{1}{2}$ (now usually called spin ladders, consisting of legs and rungs, see figure 1 for $n = 2$) have attracted considerable attention as recently reviewed by Dagotto and Rice [1]. From the theoretical point of view, these systems are intermediate between one- and two-dimensional systems. Interest in these systems started with the two-leg ladder [2] with isotropic antiferromagnetic couplings on the legs and rungs; in contrast to the $S = \frac{1}{2}$ chain this ladder is characterized by a spin gap. The appearance of this gap is immediately clear in the limit of strong ferromagnetic interactions on the rungs (it then is identical to the gap characterizing the $S = 1$ antiferromagnetic (AF) (Haldane) chain) and in the limit of interactions on the rungs only (dimer limit); the gap, however, apparently persists not only for the isotropic antiferromagnetic ladder [3–5] but for nearly all values of the coupling constants except in the limiting case of two decoupled chains. In more recent investigations, AF ladders with n legs have been shown to behave as spin liquids for n odd and as gapped systems for n even [6, 7].

Experimental investigations have been performed on the $n = 2$ ladder substance $(VO)_2P_2O_7$ [8] and also on the family of compounds $Sr_{m-1}Cu_{m+1}O_{2m}$ ($m = 3, 5, 7, \ldots$) [9] which approximately realize ladders with $n = \frac{1}{2}(m + 1)$ legs. In these materials evidence for the existence of a spin gap has been found in susceptibility [8, 9], neutron scattering [10] and magnetic resonance [11, 12] experiments. The cuprates are of additional interest as candidates for high-temperature superconductivity, which, however, remains undetected [13].

0953-8984/96/387161+17$19.50

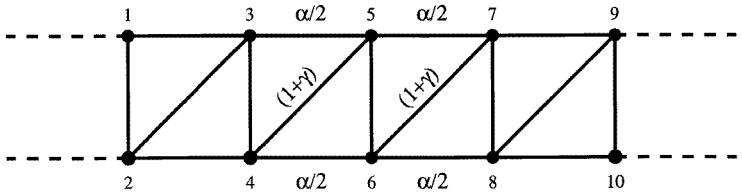

Figure 1. Structure of the generalized spin ladder with additional diagonal interaction.

These experimental results have been successfully dealt with in a large number of theoretical approaches using e.g. perturbation theory and exact numerical diagonalization [14, 15], mean-field theory based on bond operators [3] and the density matrix renormalization group approach [4, 5].

Recently theoretical interest in spin ladder models with $n = 2$ has concentrated on the fact that these models allow us to interpolate smoothly between seemingly very different spin systems when the rung coupling is varied, such as between the $S = 1$ antiferromagnetic (Haldane) chain and the dimer state, i.e. models which are built of triplets and singlets respectively on the rungs [4, 5, 16].

An interpolation between these two limiting models which avoids the singular point of two decoupled legs is possible when an additional interaction on one of the diagonal bonds is introduced as proposed by White [5] and Chitra *et al* [17]. This model is defined by the following Hamiltonian (see figure 1):

$$H = H^{(0)} + \frac{\alpha}{2}H^{(1)} + (1+\gamma)H^{(2)} \tag{1}$$

$$H^{(0)} = \sum_{j=1}^{L} \boldsymbol{S}_{1,j}\boldsymbol{S}_{2,j} \qquad H^{(1)} = \sum_{j=1}^{L}\sum_{i=1}^{2} \boldsymbol{S}_{i,j}\boldsymbol{S}_{i,j+1} \qquad H^{(2)} = \sum_{j=1}^{L} \boldsymbol{S}_{1,j}\boldsymbol{S}_{2,j+1}. \tag{2}$$

Periodic boundary conditions are used and operators $\boldsymbol{S}_{i,j}$ denote spin-$\frac{1}{2}$ operators with the indices $i = 1, 2$ labelling the two legs and $j = 1, 2 \ldots L$ labelling the L rungs. When sites are labelled by a single index (running from 1 to $2L$ as also indicated in figure 1) it becomes clear that the spin ladder with additional diagonal couplings is a generalized model composed of the spin-$\frac{1}{2}$ chains with bond alternation and next-nearest-neighbour (nnn) interaction. This model includes in particular (compare with figure 2):

- the antiferromagnetic (AF) $S = \frac{1}{2}$ Heisenberg chain with nnn exchange of relative strength $\frac{\alpha}{2}$ (α-axis, $\gamma = 0$)), including in particular the Majumdar–Ghosh (MG) limit [18] ($\alpha = 1, \gamma = 0$) with two degenerate dimerized exact ground states given as a product of singlets either on the rungs or on the diagonals;
- the AF $S = \frac{1}{2}$ Heisenberg chain with alternating exchange (γ-axis, $\alpha = 0$), including in particular the dimerized chain ($\alpha = 0, \gamma = -1$) with couplings on the rungs only and a product of singlets on the rungs as exact ground state;
- the 'regular' isotropic $S = \frac{1}{2}$ ladder for $\gamma = -1$; the experimentally relevant cases mentioned above are expected to correspond to $\alpha = 2$, i.e. to coupling of equal strength on the rungs and on the legs;
- the Haldane chain with L sites for $\gamma \to -\infty$, $\alpha > 0$ and nondiverging (leading to $S = 1$ units with an effective AF coupling $\frac{1}{4}(1+\alpha)$ on the diagonals);
- the isotropic $S = \frac{1}{2}$ AF Heisenberg chain with $2L$ sites (for $\alpha = 0, \gamma = 0$) and two decoupled AF Heisenberg chains with L sites each (for $\alpha \to \infty$ with γ finite).

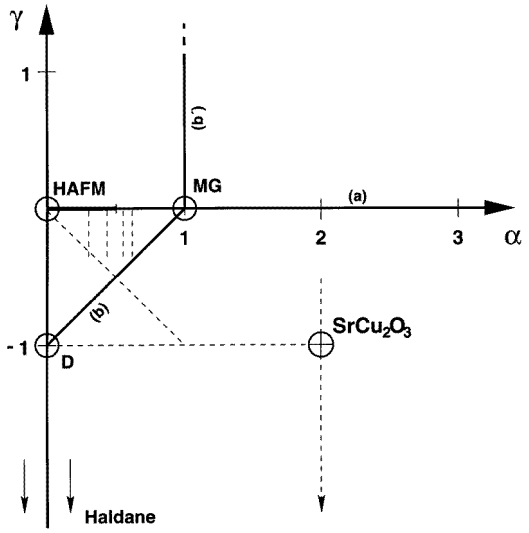

Figure 2. The phase diagram of the generalized spin ladder. Paths where numerical calculations have been performed are shown as dashed lines.

In addition the following lines in the phase diagram are of particular interest.

• The line (a), $\gamma = 0$, $\alpha \geqslant 0$, is of particular interest since on this line a transition from the gapless isotropic AF Heisenberg chain to the gapped MG chain occurs with increasing nnn coupling strength α. This transition has been investigated in detail [19, 20] (for a review see [21]) and the critical point has recently been located very accurately at $\frac{1}{2}\alpha_{cr} \approx 0.241\,167$ [22]. Line (a) and its immediate neighbourhood ($\gamma \ll 1$) is also of experimental relevance because of the discovery of the spin–Peierls compound $CuGeO_3$ with alternating and strong nnn interactions [23].

• The straight line (b), which connects the dimer point to the MG point ($(\alpha, \gamma) = (0, -1) \rightarrow (1, 0)$) is also of particular interest; on this line one of the MG ground states, the state with singlets on the rungs, remains an exact ground state [24].

In this paper we will discuss the properties of the generalized spin ladder in the space spanned by the interaction constants $\alpha > 0$ and γ. First we note that there is a symmetry transformation connecting the upper half-plane of the phase space of figure 2 to the strip $-1 < \gamma < 0$: a translation of the upper leg by one lattice constant to the left leads to a ladder with the same symmetry, but different coupling constants. The symmetry transformation exchanges the roles of rungs and diagonals; apart from a change in energy scale by a factor $1 + \gamma$ (which is qualitatively irrelevant for $\gamma > -1$), it is expressed in the following way in terms of the parameters of the Hamiltonian:

$$\gamma \rightarrow -\frac{\gamma}{1+\gamma} \qquad \alpha \rightarrow \frac{\alpha}{1+\gamma}. \tag{3}$$

The symmetry line of this transformation is the α-axis $\gamma = 0$; points on this axis are mapped onto themselves. Owing to the presence of this symmetry we will consider in the following the region $\gamma < 0$ of the α–γ-plane only. The strip $-1 < \gamma < 0$ is related to the upper half-plane by the symmetry of (3); the section $\gamma > -1$ of the α–γ-plane has AF coupling and is identical to the phase space discussed by Shastry and Sutherland [24].

Including the region $\gamma < -1$ adds the possibility of ferromagnetic coupling between the two legs; this possibility has so far been discussed for special cases only [25, 17].

In the following we will present results for the generalized spin ladder as defined by the Hamiltonian of (1) from a variational approach based on the concept of hidden order. These results will be supplemented by and compared to the results from exact diagonalizations for finite ladders with up to 14 rungs. The question of hidden order in generalized spin ladders comes up naturally since the AF $S = 1$ chain, the prototype system where hidden order emerged first, is realized in the limit $\gamma \to -\infty$. In the Haldane chain [26] hidden order has been made transparent by Kennedy and Tasaki [27], using a nonlocal unitary transformation. Ground states with complete hidden order were then written down in the form of matrix product (MP) ground states [28] and used as a basis for variational calculations. The new feature of ladders is that singlets on the rungs get mixed in when one moves from the Haldane limit $\gamma \to -\infty$ towards finite values of γ. A generalization of the Kennedy–Tasaki transformation [27] was proposed by Takada and Watanabe [29] for the isotropic spin ladder ($\gamma = -1$, varying α). Explicit definitions of hidden order in spin ladders were recently discussed by Nishiyama *et al* [30] and White [5].

Our variational approach starts from the observation that the two exact ground states of the Majumdar–Ghosh Hamiltonian can be written in the form of matrix product states. We then generalize the matrix product state to allow the *ansatz* to include the approximate ground state of the Haldane chain as given by Affleck *et al* [31] and written as a matrix product state by Klümper *et al* [28]. Continuous variation of the parameters then smoothly connects the seemingly unrelated limiting cases of the Majumdar–Ghosh and dimer points on the one hand and of the Haldane chain on the other hand. We expect this *ansatz* to make sense as a frame for a qualitative description in a large part of the half-plane $\alpha > 0$.

In section 2 we will introduce the variational matrix product states defining the hidden order in the analogous way as for an $S = 1$ chain but replacing the contribution of the $S^z = 0$ component of the rung triplet state by a linear combination of this component with the rung singlet. The exactly known ground states of the Majumdar–Ghosh chain are particular examples of this *ansatz*. This definition of matrix product states imposes a particular type of hidden order which we will describe. In section 3 we present the results of variational calculations for the ground state energy and for ground state correlation functions obtained by using this scheme. In addition the string correlation function as proposed in [5] will be computed. In section 4 we present numerical results for the ground state energy and the gap along various paths in the phase diagram (shown as dashed lines in figure 2). These results are obtained from exact diagonalization of finite ladders with up to 14 rungs and periodic boundary conditions using the Lanczos algorithm; they will be discussed in comparison to the results of the variational calculations. Our results imply that a smooth variation of parameters leads one from the Haldane phase to the dimer phase; they therefore support the hypothesis that these two limiting models are not separated by a phase transition and that the only critical behaviour in the phase diagram considered is on the gapless line $\gamma = 0, 0 < \alpha < \alpha_{cr}$. Special attention will be paid to the neighbourhood of this line in the numerical calculations. Conclusions will be given in section 5.

2. Matrix product states for spin ladders

We start by a discussion of the Majumdar–Ghosh chain, i.e. $\alpha = 1, \gamma = 0$. For periodic boundary conditions the two ground states are known exactly: they are dimerized configurations with singlets on either the rungs, $|0_r\rangle$, or the diagonal bonds, $|0_d\rangle$. If we use

the following representation of states on the jth rung:

$$|s\rangle_j = \frac{1}{\sqrt{2}}(|\uparrow\downarrow\rangle_j - |\downarrow\uparrow\rangle_j)$$
$$|t_0\rangle_j = \frac{1}{\sqrt{2}}(|\uparrow\downarrow\rangle_j + |\downarrow\uparrow\rangle_j) \qquad |t_+\rangle_j = |\uparrow\uparrow\rangle_j \qquad |t_-\rangle_j = |\downarrow\downarrow\rangle_j \tag{4}$$

the two ground states can be writen in the form of MP states

$$|0_r\rangle = \prod_{j=1}^{L} |s\rangle_j \qquad |0_d\rangle = (-1)^L \operatorname{Tr}\left(\prod_{j=1}^{L} g_j\right) \tag{5}$$

with the matrices g_j defined by

$$g_j = \frac{1}{2}\begin{pmatrix} |s\rangle_j + |t_0\rangle_j & -\sqrt{2}|t_+\rangle_j \\ \sqrt{2}|t_-\rangle_j & |s\rangle_j - |t_0\rangle_j \end{pmatrix}. \tag{6}$$

In the representation of equation (5) the MG ground states are given one in terms of singlets and one in terms of triplets on the *rungs*; this appears complicated for the state $|0_d\rangle$ but actually it serves to realize the presence of hidden order in the MG ground states. The matrix representation of the ground state according to (5) and (6) has components of the following string structure only:

$$\ldots t_+t_-t_+t_-(t_0+s)(t_0+s)\ldots(t_0+s)(t_0+s)t_+t_-t_+t_-t_+(t_0-s)(t_0-s)\ldots$$
$$(t_0-s)(t_0-s)t_-t_+t_-t_+\ldots \tag{7}$$

i.e. the sequence $\ldots t_+t_-t_+t_-\ldots$ is interrupted either by an arbitrary number of sites with $|t_0+s\rangle$ following a site with $|t_-\rangle$ or by an arbitrary number of sites with $|t_0-s\rangle$ following a site with $|t_+\rangle$.

The symmetry transformation of equation (3) transforms the ladder into itself on the line $\gamma = 0$ and the two states $|0_s\rangle$ and $|0_d\rangle$ remain degenerate for $\alpha \neq 1$; they are, however, ground states only at the Majumdar–Ghosh point. When moving off the axis $\gamma = 0$ this symmetry is destroyed and at most one of these states survives as ground state. In particular, on the line (b), $(\alpha, \gamma) = (0, -1) \to (1, 0)$, the ground state is $|0_r\rangle$, i.e. composed of rung singlets. This 'disorder line' is therefore characterized by a vanishing of the correlation length. Under the symmetry transformation (3) this line (b) transforms into the line (b′) $(\alpha, \gamma) = (1, 0) \to (1, \infty)$ with a dimerized ground state with singlets located on diagonal bonds. As discussed in the introduction it is sufficient to discuss only the region $\gamma < 0$ in the phase diagram of figure 2.

When we move away from the MG point, the state $|0_r\rangle$ has no freedom to adapt but the state $|0_d\rangle$ can be used as the basis for a variational calculation by allowing different amplitudes for the singlet and the triplet contributions. Rotational invariance requires the following form for the matrix g_j:

$$|\psi\rangle = \operatorname{Tr}\left(\prod_{j=1}^{L} g_j\right) \qquad g_j = \begin{pmatrix} a|t_0\rangle_j + b|s\rangle_j & -a\sqrt{2}|t_+\rangle_j \\ a\sqrt{2}|t_-\rangle_j & -(a|t_0\rangle_j - b|s\rangle_j) \end{pmatrix}. \tag{8}$$

This follows from the fact that the three states

$$|t^x\rangle = -\frac{1}{\sqrt{2}}(|\uparrow\uparrow\rangle - |\downarrow\downarrow\rangle) \qquad |t^y\rangle = \frac{\mathrm{i}}{\sqrt{2}}(|\uparrow\uparrow\rangle + |\downarrow\downarrow\rangle)$$
$$|t^z\rangle = \frac{1}{\sqrt{2}}(|\uparrow\downarrow\rangle + |\downarrow\uparrow\rangle) =: |t_0\rangle \tag{9}$$

form a vector and can only appear in the 2×2 matrix g_j in the combination $\sum_\alpha \sigma^\alpha |t^\alpha\rangle$ in the case of rotational invariance (σ^α are the Pauli spin matrices). In equation (8), a and b are complex variational parameters, subject to the normalization condition $3|a|^2 + |b|^2 = 1$. Thus the parameters entering the variational calculation are one amplitude and one phase.

The *ansatz* of equation (8) can be shown to reduce to the state introduced by Takada and Watanabe [29] when their state is written in original spin space (no unitary transformation) and perfect generalized hidden order is introduced. If we put $b = 0$ in equation (8) we obtain the AKLT state [31], the exact ground state of the AF $S = 1$ chain with biquadratic exchange of strength $\frac{1}{3}$.

It has to be noticed that the variational *ansatz* of equation (8) may be used with the matrices g_j defined either on the rungs or on the diagonals and as a first step of the variational calculation it is necessary to find out which of these possibilities leads to lower energy. It turns out that for $\gamma < 0$ (which is the region we will consider) lower energy is obtained when g_j is defined on the diagonals, whereas defining g_j on rungs gives the lower energy for $\gamma > 0$. On the symmetry line $\gamma = 0$ equation (8) is an approximate description of the two equivalent ground states for $\alpha_{cr} < \alpha \ll \infty$. The *ansatz* of equation (8) allows us to reproduce the exact ground state on line (b) ($\gamma = -1 + \alpha$); the variational approach is therefore exact on this line.

On the one hand, the wavefunction of equation (8) is rather general since it can smoothly interpolate between dimerized states and AKLT states, i.e. states which correspond to points which are far separated in the phase diagram. On the other hand one cannot expect this approach to work for the whole α–γ-plane since it is manifestly inadequate for special points like the ones corresponding to the HAF or to two decoupled chains, which have gapless spectra and power-law decay of correlation functions.

We finally note that there is another possibility of constructing a rotationally invariant wavefunction of the MP type which is related to the resonating valence bond structure also discussed for spin ladders: an MP wavefunction with the alternating structure

$$|0_{RVB}\rangle = \mathrm{Tr}\left(\prod_{k=1}^{\frac{L}{2}} g^+_{2k-1} g^-_{2k}\right) \qquad g^\pm_j = \frac{1}{2}\begin{pmatrix} \pm|s\rangle_j + |t_0\rangle_j & -\sqrt{2}|t_+\rangle_j \\ \sqrt{2}|t_-\rangle_j & \pm|s\rangle_j - |t_0\rangle_j \end{pmatrix} \tag{10}$$

i.e. the previous structure with diagonal elements interchanged in every second g-matrix, describes a state with singlets located on the legs. Thus our *ansatz* is also connected to RVB states on ladders as introduced in [32] and [33].

3. Variational calculations for generalized spin ladders

In this section we present the calculation of the energy, of the spin correlation function and of the string (hidden order) correlation function using the variational state of equation (8). We discuss results for these quantities in the α–γ-plane and compare to the results of alternative approximate approaches for special points. A comparison to the results of numerical calculations will be given in section 4.

The calculation of the ground state energy and of the ground state correlation functions can be done in complete analogy to the corresponding calculations for the $S = 1$ AF chain [28]. The variational energy, i.e. the expectation value of the Hamiltonian of equation (1) with the wavefunction of equation (8) and the matrix g_j defined on diagonal bonds, is

obtained as

$$\frac{E_{var}}{L} = -3\{A^4 + 2A^3B\cos\varphi + A^2B^2\cos^2\varphi\} - 3\alpha\{A^4 - A^2B^2\cos^2\varphi\} + \tfrac{3}{4}(1+\gamma)\{A^2 - B^2\} \qquad (11)$$

$$A = |a| \qquad B = |b|$$

with the norm $3A^2 + B^2 = 1$ as an additional constraint. φ is the relative phase of the original complex amplitudes a and b.

E_{var} reduces to the expression given by Watanabe [16] for $\gamma = -1$ and to the expression given by Takada and Watanabe [29] for $\gamma \to -\infty, \alpha \propto (1+\gamma)$ for perfect generalized hidden order. The procedure of minimizing E_{var} is performed easiest by first minimizing with respect to $\cos\varphi$ and then with respect to the ratio $u = B/A$. The analysis shows that the absolute minimum always corresponds to $\cos\varphi = \pm 1$, and the amplitudes a and b can always be taken as real; the remaining equation for u is of third order. Thus the minimum can be calculated exactly for general values of α and γ.

The simple variational wavefunction of equation (8) also allows the calculation of the ground state correlation functions. They exhibit the exponential decay characteristic of MP states. Owing to isotropy there is only one correlation length which is obtained as

$$\xi_{long}^{-1} = \xi_{trans}^{-1} = \ln\left(\frac{1}{|1-4A^2|}\right). \qquad (12)$$

In order to discuss the hidden order for the ladder system, we use the definition given in [5], which reproduces the known results in the $S = 1$ chain limit. Using this definition, we obtain the following result for the string correlation function (in the thermodynamic limit $L \to \infty$)

$$|g(l)| := |\langle (S^z_{2,0} + S^z_{1,1})\, \mathrm{e}^{\mathrm{i}\pi \sum_{k=1}^{l-1}(S^z_{2,k} + S^z_{1,k+1})}(S^z_{2,l} + S^z_{1,l+1})\rangle| = \tfrac{4}{9}(1-B^2)^2. \qquad (13)$$

In figure 3 we show results obtained from the MP state *ansatz* for points on the lines $\gamma = 0, -1$. In the MG case ($\gamma = 0, \alpha = 1$) and at the dimer point the variational ground state is exact; we have $A = B = \frac{1}{2}, \cos\varphi = 1$. The wavefunction is identical to that of (5) and (6), one of the two exact MG ground state wavefunctions with energy $E_{MG} = -\frac{3}{4}L$. The correlation lengths $\xi_{MG} = \xi_{dimer}$ vanish. Figures 3(a, b) shows the ground state energy and the correlation length on the lines $\gamma = 0, -1$. Discussing our results on the line $\gamma = 0$, i.e. for the general AF chain with nnn interactions, we have to restrict the discussion to the range $\alpha > \alpha_{cr} \approx 0.5$ since the MP *ansatz* is no longer appropriate when the gapless system is approached. Nevertheless we note that the variational ground state energy for $\alpha = \alpha_{cr}$ is $E_0/L = -0.793\,54$, i.e. within 1% of the exact value [17]. In the region to the right of the disorder line the relative error increases to typically 5%. The correlation lengths remain very small as is typical for MP wavefunctions.

The string order parameter is determined by the singlet weight B^2 which is shown in figure 3(c), we have $B^2 \geqslant \frac{1}{4}$ to the left and $B^2 \leqslant \frac{1}{4}$ to the right of the disorder line (b). The string order parameter for the two degenerate MG states takes the values $g_{0_r}(l) = \frac{1}{4}, g_{0_d}(l) = 0$ (obtained from $B_{0_r} = \frac{1}{2}, B_{0_d} = 1$). The fact that the string correlation is different for the two equivalent ground states is related to the asymmetric definition of the string correlation with respect to rungs and diagonals in equation (13).

For the symmetry line $\gamma = 0$, another variational wavefunction of RVB type (which is also exact at the MG point) was proposed by Zeng and Parkinson [33]. When the results for the ground state energy are compared for these two approaches, for $\alpha > 1$ lower energies are found from the RVB approach and for $\alpha < 1$ from the present MP state approach. The

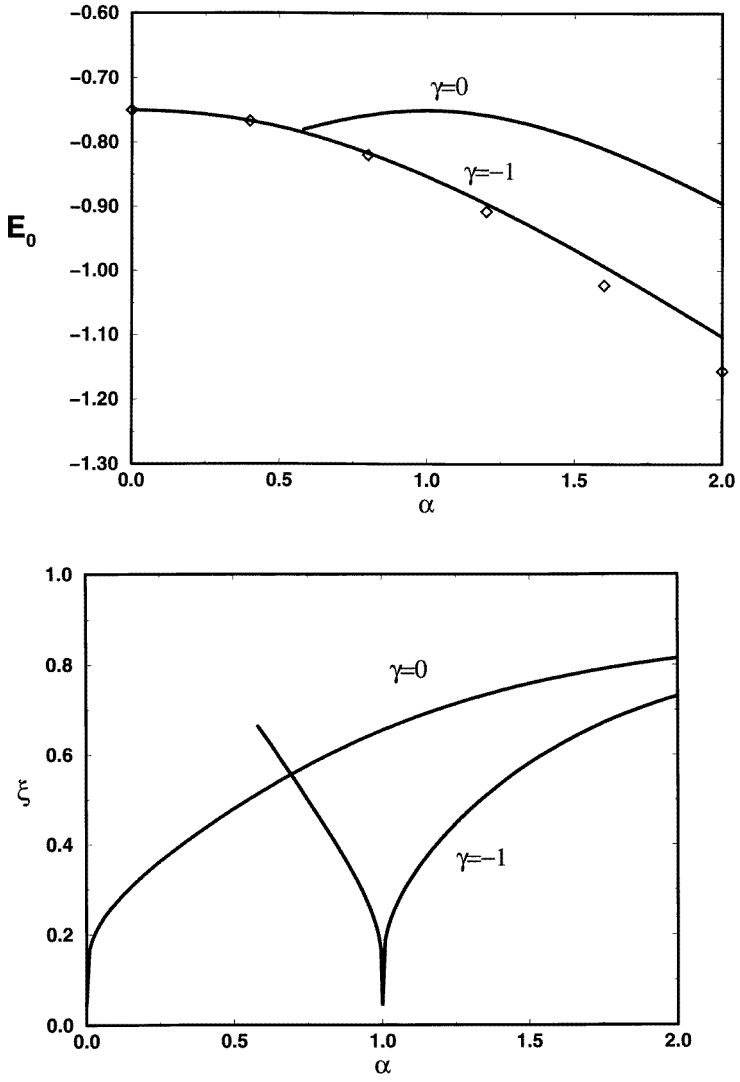

Figure 3. (a) Ground state energies, (b) correlation lengths and (c) singlet weight on the lines $\gamma = 0$ and $\gamma = -1$. Variational approach (full lines) against numerical results ($\Diamond$).

correlation length for $\alpha > 1$ is similar in the RVB and the MP state approaches, whereas for $\alpha < 1$ the MP *ansatz* results in a larger increase in ξ. The behaviour of the correlation lengths in this region of the phase diagram might be influenced by the possible emergence of a spatially modulated ground state (spiral phase) at $\alpha = 1$ [17, 33]. The MP state *ansatz* cannot by construction reproduce such a behaviour and the alternating *ansatz* as described above in equation (10) does not lead to lower variational energies either (except for large values of α). A more detailed discussion of this aspect will be given when we discuss our numerical results in section 4.

We now turn to a discussion of results for the regular ladder system ($\gamma = -1, \alpha = 2$). From the variational approach we obtain $E_0/L \approx -1.102$ and $\xi \approx 0.815$ for this isotropic

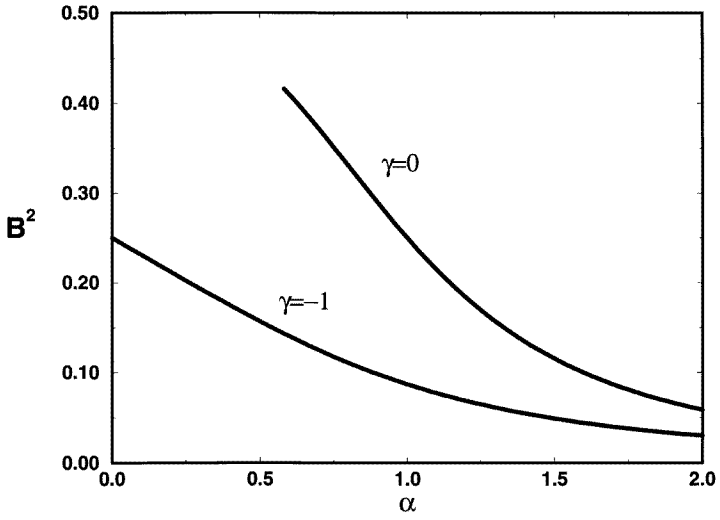

Figure 3. (Continued)

ladder. These results may be compared to those for a variational RVB wavefunction which was proposed by Fan and Ma [34] and leads to a ground state energy of $E_0/L \approx -1.112$ and a correlation length of $\xi \approx 0.238$. The difference between the two variational energies of about 1% appears negligible when it is compared to the exact (numerical) result $E_0/L \approx -1.156$. Both variational methods lead to correlation lengths considerably smaller than $\xi \approx 3.19$ as computed in [32]. This is consistent with the well known fact that in approaches using MP states the correlation length is notoriously underestimated (compare the AKLT value of $\xi \approx 0.9102$ to the exact correlation length $\xi \approx 6.2$ in the AF $S = 1$ chain).

Finally we want to illustrate in figures 4(a)–(c) how the limit of an antiferromagnetic $S = 1$ chain is included in the present scheme for $\gamma \to -\infty$. In this limit it is very unfavourable to have singlets on the diagonal bonds, so minimization leads to $B \to 0$. We show the ground state energy and the singlet weight with increasing $|\gamma|$ for $\alpha = 2$ in figure 4(a) and in figure 4(c) respectively. Combining these graphs with the corresponding ones from figure 3 we can follow a continuous path from the dimer point to the Haldane limit. The smooth variation of the physical quantities on such a path illustrates the similarity of the Haldane phase and the dimer phase in the present approach.

The minimum of the variational energy in the limit appropriate for the AF $S = 1-$ chain has the following form

$$E_0^{S=1} = \lim_{\gamma \to -\infty} E_0 \approx \left(\frac{1+\gamma}{4} - \frac{\alpha+1}{3} + \frac{1}{3(1+\gamma)} \right) L \qquad (|1+\gamma| \gg 1)$$
$$B^2 \approx \frac{1}{3(1+\gamma)^2}. \tag{14}$$

The first term in $E_0^{S=1}$ is just the internal energy of the triplets representing the internal energy of spins $S = 1$ at the L sites. We see that minimization in the limit of infinite negative γ leads to the AKLT state with

$$A^2 = \tfrac{1}{3} \qquad E_0 = -\tfrac{4}{3} J_{eff} \qquad J_{eff} = (\alpha+1)/4. \tag{15}$$

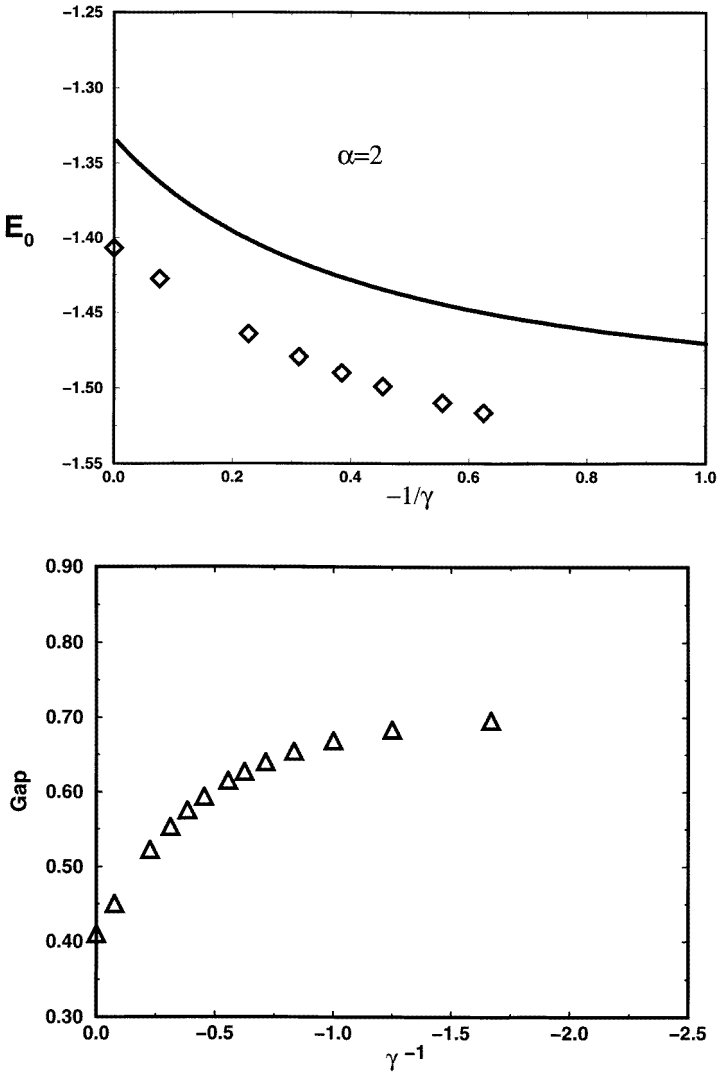

Figure 4. Approach to the Haldane limit on the line $\alpha = 2$: (a) ground state energy, (b) gap energy, (c) singlet weight, (d) characteristic length L_0.

This is the identical result as obtained from direct variational calculations for the $S = 1$ chain [27].

For the $S = 1$ chain the hidden order is characterized by the string order parameter as introduced in [35]. In our approach, the AKLT value $g(\infty) = \frac{4}{9}$ is reproduced in the limit of zero singlet weight, i.e. for $B = 0$. As is seen from the monotonic behaviour of the singlet weight in figure 4(c) in combination with equation (13), the string order parameter $g(\infty)$ decreases monotonically when γ is increased from $-\infty$ towards 0.

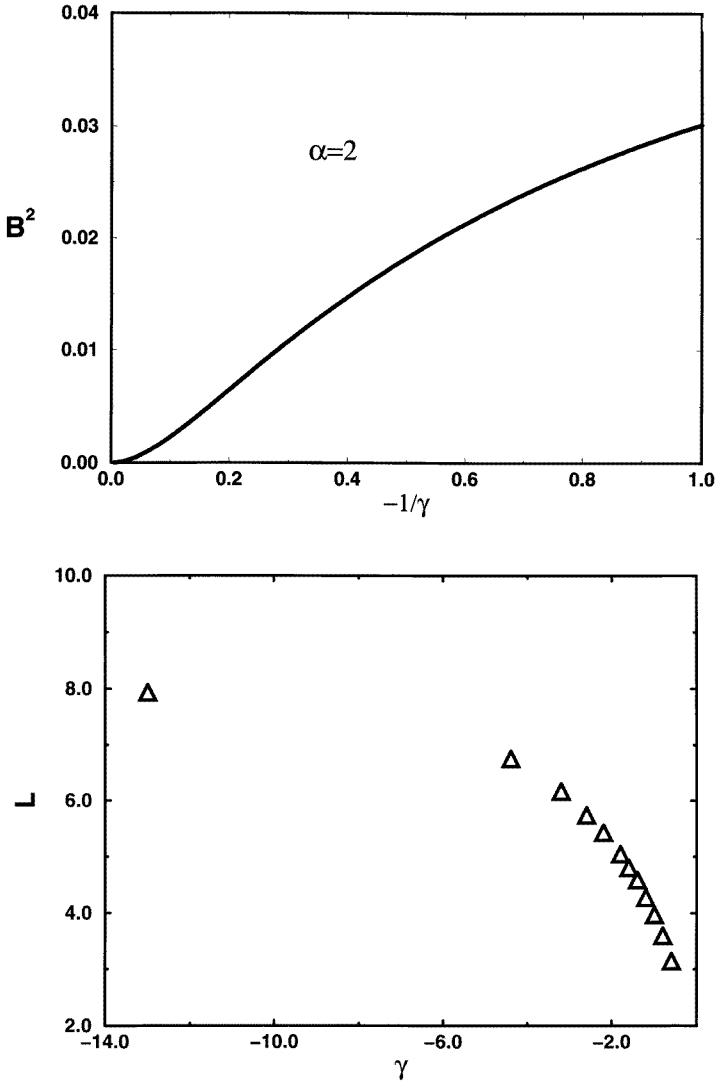

Figure 4. (Continued)

4. Numerical Results

We have computed the ground state energy per rung and the energy gap for different values of the nnn interaction α and the alternating bond exchange γ in order to compare these exact results to those obtained in the variational calculation of the last section in the various regions of the phase diagram. The paths which we have investigated numerically are shown in figure 2 as dashed lines. The results for points in the upper half plane follow from the symmetry property given in equation (3).

Numerical calculations were done on the MPP Cray T3D SC256 of the Zuse Computing Centre Berlin. We used the Lanczos technique to determine the ground state energy *per rung* as well as the singlet–triplet energy gap on $2 \times L$ lattices for $L = 6, 8, 10, 12, 14$. In

order to extrapolate the results for finite L to the bulk limit we used the *ansatz* of [14],

$$f(L) = f(\infty) + c_0\, \mathrm{e}^{-L/L_0}\, L^{-p} \tag{16}$$

i.e. a power law in L multiplied by an exponential. Following [14] the Lanczos data were fitted using $p = 2$ for the ground state energy per rung and $p = 1$ for the gap energy. The typical relative mean square error of these fits was about 10^{-10} for the ground state energy and about 10^{-7} for the gap energy. The fit parameter L_0 reflects the characteristic length of the system and corresponds to the correlation length in the chain under consideration. We have checked the accuracy of our program by recalculating data for the isotropic ladder ($\alpha = 2, \gamma = -1$) and have fully reproduced the results of [14].

In our numerical calculations we have concentrated on two different aspects of generalized spin ladders:

- on the variation of the ground state energy and of the excitation gap when we move from the dimer state to the Haldane limit (these data allow us to estimate quantitatively the accuracy of the variational approach based on MP states and to discuss the issue of whether these two limiting states are separated by a phase boundary) and
- on the neighbourhood of the gapless line (a) connecting the two conformal points $\gamma = 0$, $\alpha = 0$ (HAFM) and $\gamma = 0$, $\alpha = \alpha_{cri} \approx 0.5$. Such data are expected to contribute to an understanding of the crossover from the gapless phase on the critical line $\gamma = 0$, $\alpha < \alpha_{cr}$ to the gapped phase(s) of the MG/dimer and Haldane type.

We present the variations of the ground state energy, the gap energy and the length L_0 from the dimer point to the Haldane limit on the paths shown as dashed lines in figure 2. Our numerical results for various chain lengths and their extrapolation to the bulk limit are given in tables 1 and 2 and displayed in figures 3 and 4. An extrapolation to the limit $\gamma \to -\infty$ was performed with a fourth-order polynomial fit to $E_0/L - (1+\gamma)/4$ for the points $\alpha = 2$, $\gamma = -2.2, -2.6, -3.2, -4.4, -13$. This extrapolation resulted in

$$\frac{1}{J_{eff}}\left(\frac{E_0}{L} - \frac{1+\gamma}{4}\right) \approx -1.4069 \qquad \frac{1}{J_{eff}}\,\Delta \approx 0.4106 \tag{17}$$

with $J_{eff} = (\alpha+1)/4 = \frac{3}{4}$. Both numbers are in excellent agreement with the well known results for the ground state energy and the gap of the Haldane chain [36]. The analogous extrapolation for the characteristic length L_0 (see equation (16)) is shown in figure 4(d); L_0 increases monotonically when we approach the Haldane limit on our path. The variation of L_0 corresponds to the variation of the correlation length ξ although the limiting value of L_0 is found to be somewhat larger than the accepted numerical value for the correlation length of the Haldane chain $\xi \approx 6.2$.

The numerical results are in agreement with the observation already made for the variational results: on the continuous path through the phase diagram the quantities E_0, Δ, L_0 vary smoothly and there is no indication of a phase boundary in the variation of these quantities. These data therefore support the hypothesis that the dimer point, the Majumdar–Ghosh point and the Haldane limit all are in the same phase. The gap characterizing these three limiting chains as well as the intermediate systems, including the regular spin ladder, thus appears to be only quantitatively different and these systems therefore should be considered as manifestation of basically the same quantum condensation phenomenon.

We now turn to the second region of interest in the phase diagram, the area around the line of vanishing gap connecting the two known conformal points. We calculated the energies of the ground state and of the first excited states

Table 1. Ground state energy E_0 and gap energy $\Delta_{k=\pi}$ for $\alpha = 2$ and various values of γ.

	Ground state energy					
γ	$N = 12$	$N = 16$	$N = 20$	$N = 24$	$N = 28$	$N \to \infty$
−1.0	−1.168 874	−1.160 406	−1.157 719	−1.156 744	−1.156 363	−0.578 020
−2.2	−1.442 089	−1.431 225	−1.427 342	−1.425 759	−1.425 061	−0.712 146
−2.6	−1.536 390	−1.525 068	−1.520 950	−1.518 238	−1.518 469	−0.758 797
−3.2	−1.679 514	−1.667 673	−1.663 286	−1.661 423	−1.660 568	−0.829 772
−4.4	−1.969 666	−1.957 152	−1.952 409	−1.950 343	−1.949 366	−0.974 069
−13.0	−4.095 278	−4.081 498	−4.073 567	−4.073 567	−4.072 326	−2.035 283
$\gamma \to -\infty$						$-(\gamma + 1)/4 - 0.527\,59$
	Gap					
γ	$N = 12$	$N = 16$	$N = 20$	$N = 24$	$N = 28$	$N \to \infty$
−1.0	0.626 569	0.557 398	0.528 107	0.514 784	0.508 496	0.501 711
−2.2	0.605 725	0.527 135	0.489 590	0.470 340	0.460 095	0.445 421
−2.6	0.600 401	0.519 686	0.480 410	0.459 877	0.448 724	0.431 682
−3.2	0.593 758	0.510 573	0.469 294	0.447 250	0.435 003	0.415 168
−4.4	0.583 965	0.497 512	0.453 582	0.429 489	0.415 715	0.391 956
−13.0	0.559 096	0.466 436	0.417 295	0.389 032	0.371 958	0.337 796
$\gamma \to -\infty$						0.307 97

Table 2. Ground state energy E_0 and gap energy $\Delta_{k=\pi}$ for $\gamma = -1$ and various values of α.

	Ground state energy					
α	$N = 12$	$N = 16$	$N = 20$	$N = 24$	$N = 28$	$N \to \infty$
0.0						0.75
0.4	0.766 403	0.766 398	0.766 398	0.766 3978	0.766 3978	0.766 3978
0.8	0.819 531	0.819 281	0.819 256	0.819 254	0.819 253	0.819 253
1.2	0.909 511	0.907 827	0.907 510	0.907 443	0.907 428	0.907 424
1.6	1.029 126	1.024 466	1.023 234	1.022 867	1.022 749	1.022 687
	Gap					
α	$N = 12$	$N = 16$	$N = 20$	$N = 24$	$N = 28$	$N \to \infty$
0.0						1.0
0.4	0.821 753	0.821 709	0.821 707	0.821 707	0.821 707	0.821 707
0.8	0.692 602	0.690 373	0.690 074	0.690 032	0.690 026	0.690 025
1.2	0.619 862	0.605 463	0.601 817	0.600 848	0.600 582	0.600 482
1.6	0.602 390	0.563 670	0.549 962	0.544 825	0.542 838	0.541 330

- for $0.3 < \alpha < 0.6$ and small values of γ, allowing an extrapolation to $\gamma = 0$
- for values on the line $\gamma = -\alpha$, i.e. on a path from the gapless HAF towards the gapped phase at larger values of α, γ.

In figure 5 and in table 3 we show the behaviour of the gap when the gapless line, $\gamma = 0$, is approached, i.e. the vanishing of the gap on the critical line and the (small) finite gap energy for $\alpha > \alpha_{cr}$. For $|\gamma| \ll 1$ and two values of $\alpha < \alpha_{cr}$ we have analysed the results assuming a power law behaviour, $\Delta \propto |\delta|^{\nu}$ (where $\delta = \gamma/(2+\gamma)$ is the dimerization

parameter), in order to compare with the prediction $y = \frac{2}{3}$ by Cross and Fisher [37]. From a log–log plot (see inset in figure 5) we find $y \approx 0.862$ for $\alpha = 0.30$ and $y \approx 0.795$ for $\alpha = 0.44$, i.e. an α-dependent exponent which is somewhat larger than predicted in [37].

Table 3. Gap energy $\Delta_{k=0}$ close to the gapless line (a).

	Gap energy				
α	$\gamma = 0.90$	$\gamma = 0.95$	$\gamma = 0.97$	$\gamma = 0.985$	$\gamma = 1.00$
0.30	0.251 1807	0.149 7976	0.097 1629	0.052 6672	0.000 03
0.44	0.279 9086	0.172 0255	0.116 7782	0.066 0249	0.000 03
0.52	0.300 2298	0.186 4918	0.131 0506		0.000 9896
0.6	0.325 1090	0.208 2006	0.150 7519		0.002 3626

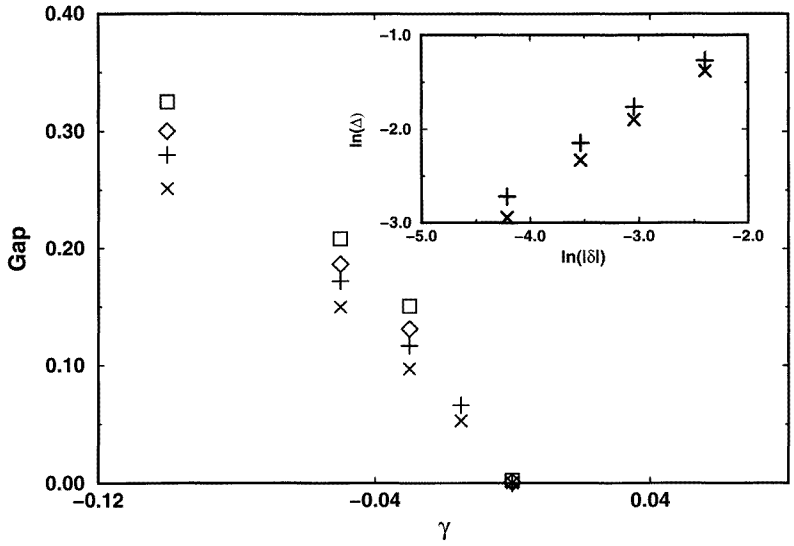

Figure 5. γ-dependence of the energy gap $\Delta_{k=0}$ close to the gapless line (a): $\alpha = 0.30$ (+), 0.44 (×), 0.52 (◇), 0.60 (□). Inset: scaling of the gap with the dimerization parameter $\delta = \gamma/(2+\gamma)$ for $\alpha = 0.30, 0.44$.

The gap close to the conformal line is found at wavevector $k = 0$, whereas the gap in the Haldane phase is known to occur at wavevector $k = \pi$ (the wavevector k is defined through the factor $\exp(ik)$ which multiplies the wavefunction upon the transformation $j \to j + 1$, i.e. a shift of rungs by one unit). To discuss this crossover in the wavevector of the lowest excitation we have calculated the lowest excitation energies for these two wavevectors, $\Delta_{k=0}$, $\Delta_{k=\pi}$ along the path $\gamma = -\alpha$. The results of an extrapolation to the thermodynamic limit as described above are shown in figure 6. It is seen that the quantity $\Delta_{k=0} - \Delta_{k=\pi}$ changes sign for $\alpha \approx 0.55$ i.e. close to the line $\gamma = -1 + \alpha$ which connects the dimer and MG points. These results for the gap (and the corresponding results for the ground state energy) join smoothly to the results presented before when values $\alpha = 2$ are reached. Actually the excitation energies on the disorder line $\gamma = -1 + \alpha$ can be calculated in

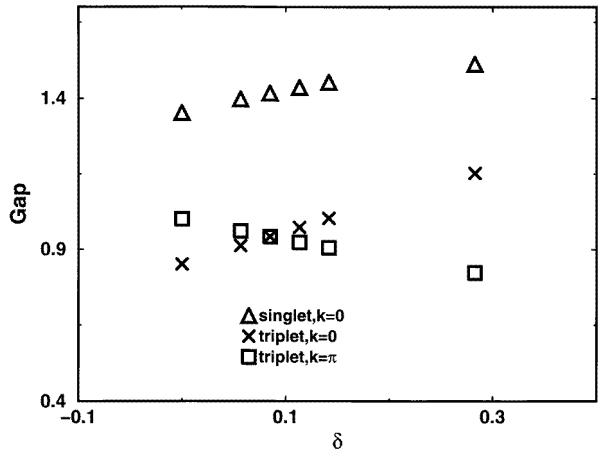

Figure 6. Energy gaps $\Delta_{k=0}$ and $\Delta_{k=\pi}$ along the line $\gamma = -\alpha$. $\delta = (\alpha^2 + \gamma^2)^{1/2}$.

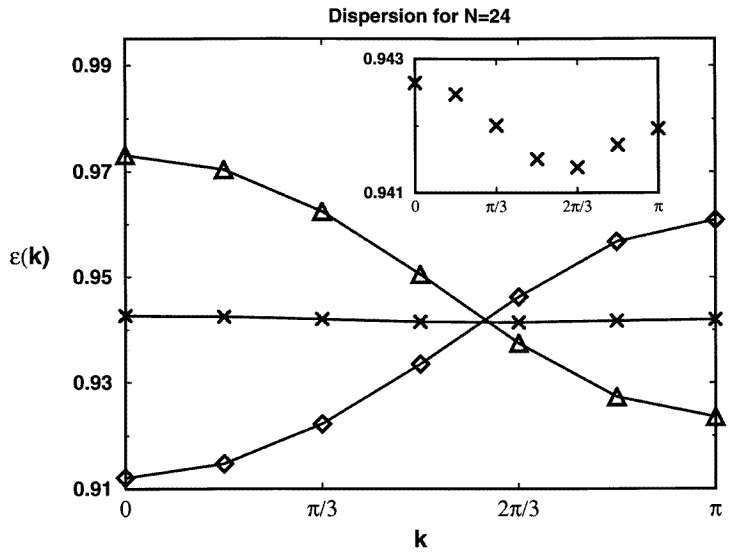

Figure 7. Excitation spectra $\epsilon(k)$ close to the disorder line, $-\gamma = \alpha = 0.54$ ($\Diamond$), 0.56 ($\times$), 0.58 ($\triangle$) for $L = 12$. Inset: expanded scale for $-\gamma = \alpha = 0.56$. Full lines are guides to the eye.

perturbation theory in α to a high degree of accuracy for $\alpha \ll 1$. For $k = \pi$ we have the exact result $\Delta_{k=\pi} = 1$ on the whole disorder line, as will be published elsewhere.

Generally, our numerical results confirm the variational results in that variations over most of the phase diagram are smooth and do not indicate any phase boundaries. However, we find that the excitation spectrum does change qualitatively along a path from the critical line to the gapped phase; this may be another aspect of the fact that the maximum of the structure factor $S(k)$ is found at finite k and may be related to the existence of a spiral phase as speculated before [33, 17]. In order to clarify this point, more detailed results on the excitation spectrum in this region of the phase diagram should be obtained. However, since a reliable finite-size analysis is not possible for general values of the wavevector we

cannot discuss the character of the complete excitation spectrum with comparable accuracy and therefore cannot decide whether the minimum excitation energy occurs at some finite value of the wavevector. In order to provide some preliminary information we present in figure 7 the excitation spectrum for the finite ladder with 2×12 sites at the points $\alpha = -\gamma = 0.54, 0.56, 0.58$. The minimum excitation energy is found at $k = 0$ for $\alpha = -\gamma = 0.54$, at $k = \pi$ for $\alpha = -\gamma = 0.58$. For $\alpha = -\gamma = 0.56$ the minimum is found at finite wavevector, $k \approx 2\pi/3$, although dispersion is very weak and it is not clear whether the minimum at finite wavevector will survive an appropriate extrapolation to the infinite system. Actually, this result may be more accurate than one might expect from the small size of the system since we found in the finite-size extrapolations for $k = 0, \pi$ that the results for the finite 2×12 site system differ very little (relative difference 10^{-6}) from the thermodynamic limit. For a full understanding more calculations are clearly required.

5. Conclusions

We have investigated the phase diagram of a generalized spin ladder with additional interaction on diagonal bonds. This model includes several known cases, in particular the $S = 1$ chain in the Haldane phase and the dimer and Majumdar–Ghosh chains belonging to a dimerized phase. This generalized spin ladder was studied with a variational wave *ansatz* and numerical techniques. Using the concept of hidden order throughout the whole phase diagram (with the exception of the line of gapless points), a rotationally invariant matrix product state was proposed for the ground state of these ladders. The ground state energy, and spin and string correlations, were calculated. The comparison with numerical results for the ground state energies leads to agreement typically within about 4–5%, consistent with the qualitative nature of our approximation. In the $S = 1$ chain limit the well known AKLT state and the variational energy of $\frac{4}{3}$ per site are reproduced and extrapolation of the numerical results leads to excellent agreement with the known values for the ground state energy and the gap of the Haldane chain. A string correlation function was chosen such as to reproduce in the corresponding limit the AKLT value of $\frac{4}{9}$ for the factorizing approximation to the $S = 1$ chain. This string correlation function is directly related to the singlet weight in the MP wavefunction and decreases monotonically when one moves from the Haldane limit towards dimerized states.

From both the numerical and the variational calculations we find on paths connecting the dimer and Majumdar–Ghosh points to the Haldane limit smooth variations of all quantities considered. We are therefore led to conclude that these dimerized AF $S = \frac{1}{2}$ chains and the AF $S = 1$ chain are in the same phase and that the gap in the excitation spectrum of these chains is of the same nature. On the other hand, our numerical data for the excitation spectrum close to the line connecting the dimer and the MG points show a shift of the wavevector of the minimum excitation energy from $k = 0$ to $k = \pi$ as well as an indication that the minimum may be found at intermediate wavevectors. Thus the question of the existence of a chiral phase remains unresolved and requires further investigation.

Using the present approach elementary excitations can be constructed as soliton-like states as for dimer-like systems [24] and for the $S = 1$ chain [38]. Our approach can also be extended to include anisotropic couplings; in particular, similar as in the AF $S = 1$ chain, there should be a critical value for the Ising-like anisotropy on the legs, at which the system exhibits long-range order even for $\gamma \to -\infty$. These further applications of the MP approach are now under investigation.

Acknowledgments

We gratefully acknowledge useful discussions with A Kolezhuk, B Lüthi and C Waldtmann. This work was supported by the German Federal Ministry of Research and Technology (BMBF) under contract number 03-MI4HAN-8. The numerical calculations were performed at the Regionales Rechenzentrum Niedersachsen and Zuse Rechenzentrum Berlin, we wish to thank these institutions for their helpful cooperation.

References

[1] Dagotto E and Rice T M (1996) *Science* **271** 618
[2] Hirsch R 1988 *Thesis* Universität Köln
[3] Gopalan S, Rice T M and Sigrist M 1994 *Phys. Rev.* B **49** 8901
[4] Hida K 1991 *J. Phys. Soc. Japan* **60** 1347, 1939; 1995 *Preprint*
[5] White S R 1996 *Phys. Rev.* B **53** 52
[6] Frischmuth B, Ammon B and Troyer M *Preprint* condmat/9601025
[7] Hatano N and Nishiyama Y 1995 *J. Phys. A: Math. Gen.* **28** 3911
[8] Johnston D C, Johnson J W, Goshorn D P and Jacobson A J 1987 *Phys. Rev.* B **35** 219
[9] Hiroi Z, Azuma M, Takano M and Bando Y 1991 *J. Solid State Chem.* **95** 230
[10] Eccleston R S, Barnes T, Brody J and Johnson J W 1994 *Phys. Rev. Lett.* **73** 2626
[11] Matsuda M and Katsumata K 1995 *Preprint*
[12] Schwenk H, Sieling M, König D, Palme W, Svyagin S A, Lüthi B and Eccleston R S 1996 *Preprint*
[13] Hiroi Z and Takano M 1995 *Nature* **377** 41
[14] Barnes T, Dagotto E, Riera J and Swanson E S 1993 *Phys. Rev.* B **47** 3196
[15] Barnes T and Riera J 1994 *Phys. Rev.* B **50** 6817
[16] Watanabe H 1995 *Phys. Rev.* B **52** 12 508
[17] Chitra R, Pati Swapan, Krishnamurthy H R, Sen Diptiman and Ramasesha S 1995 *Phys. Rev.* B **52** 6581
[18] Majumdar C K and Ghosh D K 1969 *J. Math. Phys.* **10** 1399
[19] Haldane F D M 1982 *Phys. Rev.* B **25** 4925
[20] Tonegawa T and Harada I 1987 *J. Phys. Soc. Japan* **56** 2153
[21] Harada I and Tonegawa T 1993 *Recent Advances in Magnetism of Transition Metal Compounds* ed A Kotani and N Suzuki (Singapore: World Scientific)
[22] Eggert S *Preprint* cond-mat/9602026
[23] Castilla G, Chakravarty S and Emery V J 1995 *Phys. Rev. Lett.* **75** 1823
[24] Shastry B S and Sutherland B 1981 *Phys. Rev. Lett.* **47** 964
[25] Watanabe H 1994 *Phys. Rev.* B **50** 13 442
[26] Haldane F D M 1983 *Phys. Rev. Lett.* **50** 1153
[27] Kennedy T and Tasaki H 1992 *Phys. Rev.* B **45** 304
[28] Klümper A, Schadschneider A and Zittartz J 1993 *Europhys. Lett.* **24** 293
[29] Takada S and Watanabe H 1992 *J. Phys. Soc. Japan* **61** 39
[30] Nishiyama Y, Hatano N and Suzuki M 1995 *J. Phys. Soc. Japan* **64** 1967
[31] Affleck I, Kennedy T, Lieb E and Tasaki H 1987 *Phys. Rev. Lett.* **59** 799; 1988 *Commun. Math. Phys.* **115** 583
[32] White S R, Noack R M and Scalapino D J 1994 *Phys. Rev. Lett.* **73** 886
[33] Zeng C and Parkinson J B 1995 *Phys. Rev.* B **51** 11 609
[34] Fan Y and Ma M 1988 *Phys. Rev.* B **37** 1820
[35] Rommelse K and den Nijs M 1987 *Phys. Rev. Lett.* **59** 2578
[36] Golinelli O, Jolicoeur Th and Lacaze R 1994 *Phys. Rev.* B **50** 3037
[37] Cross M C and Fisher D S 1979 *Phys. Rev.* B **19** 402
[38] Neugebauer U and Mikeska H J 1996 *Z. Phys.* B **99** 151